Ginsenoside Rg3 Enhances Large Conductance Ca2+-Activated Potassium Channel Currents: A Role of Tyr360 Residue

Sun-Hye Choi[1,4], Tae-Joon Shin[1,4], Byung-Hwan Lee[1,4], Sung Hee Hwang[1], Sang-Mok Lee[1], Byung-Cheol Lee[2], Cheol-Seung Park[2], Tal Soo Ha[3], and Seung-Yeol Nah[1,*]

Ginsenosides, active ingredients of *Panax* ginseng, are known to exhibit neuroprotective effects. Large-conductance Ca^{2+}-activated K^+ (BK_{Ca}) channels are key modulators of cellular excitability of neurons and vascular smooth muscle cells. In the present study, we examined the effects of ginsenosides on rat brain BK_{Ca} (*rSlo*) channel activity heterologously expressed in *Xenopus* oocytes to elucidate the molecular mechanisms how ginsenoside regulates the BK_{Ca} channel activity. Ginsenoside Rg3 (Rg3) enhanced outward BK_{Ca} channel currents. The Rg3-enhancement of outward BK_{Ca} channel currents was concentration-dependent, voltage-dependent, and reversible. The EC_{50} was 15.1 ± 3.1 μM. Rg3 actions were not desensitized by repeated treatment. Tetraetylammonium (TEA), a K^+ channel blocker, inhibited BK_{Ca} channel currents. We examined whether extracellular TEA treatment could alter the Rg3 action and *vice versa*. TEA caused a rightward shift of the Rg3 concentration-response curve (i.e., much higher concentration of Rg3 is required for the activation of BK_{Ca} channel compared to the absence of TEA), while Rg3 caused a rightward shift of the TEA concentration-response curve in wild-type channels. Mutation of the extracellular TEA binding site Y360 to Y360I caused a rightward shift of the TEA concentration-response curve and almost abolished both the Rg3 action and Rg3-induced rightward shift of TEA concentration-response curve. These results indicate that Tyr360 residue of BK_{Ca} channel plays an important role in the Rg3-enhancement of BK_{Ca} channel currents.

INTRODUCTION

Large-conductance Ca^{2+}-activated K^+ (BK_{Ca}) channels are a family of potassium-selective ion channels activated in response to elevation of intracellular free Ca^{2+} level following membrane depolarization (Hille, 2001). BK_{Ca} channels are composed of two subunits: the α (also called *Slo*) subunit, which forms the channel pore (Ghatta et al., 2006; Salkoff et al., 2006), and the β subunit (Wanner et al., 1999), which modifies the voltage and calcium sensitivity of the pore-forming subunit (Qian et al., 2002). The α subunit has large cytoplasmic C terminus, is responsible for the calcium-dependent activation of the channel (Fig. 1B) (Schreiber and Salkoff, 1997; Schreiber et al., 1999; Wei et al., 1994), and is activated by increased intracellular Ca^{2+} and/or Ca^{2+}-dependent kinases including CaM kinases, PKA, and PKC (Toro et al., 1998; Weiger et al., 2002). BK_{Ca} channels play key roles in a variety of neuronal and non-neu-ronal cell functions. For example, in neurons, BK_{Ca} channels regulate frequency of firing, action potential afterhyperpolarization and neurotransmitter release. BK_{Ca} channels are also one of the main ion channels that contribute action potential repolarization and afterhyperpolarization during excitation-contraction coupling in vascular smooth muscle cells (Ohi et al., 2001).

Ginseng, the root of *Panax* ginseng C.A. Meyer, has been used as a representative tonic or an adaptogen to promote longevity and enhance bodily functions against hypertension and various ailments for several hundred years in Far Eastern countries. Recent reports have shown that ginsenosides, one of the active ingredients in ginseng, inhibit ion channels that are involved in neuronal excitabilities such as voltage-dependent Ca^{2+} and Na^+ channels (Fig. 1A) (Choi et al., 2009; Lee et al., 2005). BK_{Ca} channels are usually co-localized with voltage-dependent Ca^{2+} channels (Berkefeld et al., 2006). Little is known about ginsenoside effects on BK_{Ca} channel activities.

In the present study, we examined ginsenoside effects on rat brain BK_{Ca} (*rSlo*) channel activities expressed in *Xenopus* oocytes using the two-electrode voltage clamp and outside-out patch clamp techniques (Ha et al., 2006; Lu et al., 1990). We demonstrated that among various ginsenosides Rg3 most potently enhanced BK_{Ca} channel currents and that this action was concentration- and voltage-dependent and reversible. However, site-directed mutagenesis of the channel pore entry site greatly attenuated Rg3 action. In this communication, we present results suggesting that the Y360 residue in the channel pore entry site is involved in Rg3-mediated enhancement of the BK_{Ca} channel currents.

MATERIALS AND METHODS

Materials

Ginsenosides were provided by AMBO Institute (Korea) (Fig. 1A). We used the cDNAs for rat brain BK_{Ca} channel (GenBank No. NM_000218) that were previously reported (Ha et al., 2006). All other reagents were purchased from Sigma-Aldrich (USA).

Preparation of *Xenopus* oocytes and microinjection

Xenopus laevis frogs were purchased from Xenopus I (Ann Arbor, USA). Their care and handling were in accordance with the highest standards of institutional guidelines of Konkuk University. For isolation of oocytes, frogs were anesthetized with an aerated solution of 3-amino benzoic acid ethyl ester followed by removal of ovarian follicles. The oocytes were treated with collagenase and then agitated for 2 h in Ca^{2+}-free OR2 medium containing 82.5 mM NaCl, 2 mM KCl, 1 mM $MgCl_2$, 5 mM HEPES, 2.5 mM sodium pyruvate, 100 units/ml penicillin and 100 μg/ml streptomycin. Stage V-VI oocytes were collected and stored in ND96 medium (in mM: 96 NaCl, 2 KCl, 1 $MgCl_2$, 1.8 $CaCl_2$, and 5 HEPES, pH 7.5) supplemented with 50 μg/ml gentamicin. The oocyte-containing solution was maintained at 18°C with continuous gentle shaking and renewed daily. Electrophysiological experiments were performed within 5-6 days of oocyte isolation, with ginsenoside applied to the bath. For BK_{Ca} channel experiments, BK_{Ca} channel-encoding cRNAs (40 nl) were injected into the animal or vegetal pole of each oocyte one day after isolation, using a 10 μl microdispenser (VWR Scientific, USA) fitted with a tapered glass pipette tip (15-20 μm in diameter) (Lee et al., 2008).

Site-directed mutagenesis of the BK_{Ca} α and *in vitro* transcription of BK_{Ca} channel cDNAs

Single amino acid substitutions of BK_{Ca} channel (Fig. 1B) were made using a QuikChange™ XL Site-Directed Mutagenesis Kit (Stratagene, USA), along with Pfu DNA polymerase, in addition to sense and antisense primers encoding the desired mutations. Overlap extension of the target domain by sequential polymerase chain reaction (PCR) was carried out according to the manufacturer's protocol. The final PCR products were transformed into *E. coli* strain DH5α, screened by PCR and confirmed by sequencing of the target regions. The mutant DNA constructs were linearized at their 3′ ends by digestion with *Not*I, and run-off transcripts were prepared using the methylated cap analog, $m^7G(5')ppp(5')G$. The cRNAs were prepared using a mMessage mMachine transcription kit (Ambion, USA) with T7 RNA polymerase. The absence of degraded RNA was confirmed by denaturing agarose gel electrophoresis followed by ethidium bromide staining. Similarly, recombinant plasmids containing rat BK_{Ca} channel cDNA inserts were linearized by digestion with the appropriate restriction enzymes, and cRNAs were obtained using the mMessage mMachine *in vitro* transcription kit (Ambion, USA) with SP6 RNA polymerase or T7 polymerase. The final cRNA products were resuspended at a concentration of 1 μg/μl in RNase-free water, and stored at -80°C (Lee et al., 2008).

Data recording

Data recording for BK_{Ca} channel currents were performed as described by Lu et al. (1990). A custom-made Plexiglas net chamber was used for two-electrode voltage-clamp recordings as previously reported. The oocytes were impaled with two microelectrodes filled with 3 M KCl (0.2-0.7 MΩ), and electrophysiological experiments were carried out at room tempera-

ture using an Oocyte Clamp (OC-725C, Warner Instruments, USA). Stimulation and data acquisition were controlled with a pClamp 8 (Axon Instruments, USA). For most electrophysiological experiments, oocytes were perfused initially with Cl⁻- and Ca^{2+}-free solution (in mM: 96 NaOH, 2 KOH, 8 Mg-gluconate, 5 HEPES, 5 EGTA, pH 7.4 with methanesulfonic acid) in the presence of Cl⁻ channel blocker (500 μM anthracene-9-carboxylic acid) (Lu et al., 1990) to inhibit endogenous Cl⁻ channels. The oocytes were then clamped at a holding potential of -80 mV, membrane potential was depolarized to +40 mV for 400 ms at 10 s intervals, and currents were recorded as otherwise indicated.

All macroscopic current recordings were performed using the gigaohm-seal patch-clamp method in an outside-out configuration (Hamil et al., 1981). Patch pipettes were fabricated from borosilicate glass (WPI, USA) and were fire-polished to a resistance of 5-7 MΩ. The channel currents were amplified using an Axopatch 200B amplifier (Axon Instruments, USA), low-pass filtered at 1 or 2 kHz using a four-pole Bessel filter, and digitized at a rate of 10 or 20 points/ms using a Digidata 1200A apparatus (Axon Instruments). The macroscopic currents of expressed channels were activated by voltage-clamp pulses delivered from a holding potential of -100 mV to membrane potentials ranging from -80 to 200 mV in 10 mV increments. The intracellular and extracellular solutions contained the following components, unless otherwise specified: 116 mM KOH, 4 mM KCl, 10 mM HEPES, and 5 mM EGTA at pH 7.2.

To provide the precise free concentration of intracellular Ca^{2+} ($[Ca^{2+}]_i$), the appropriate amount of total Ca^{2+} to be added to the intracellular solution was calculated using the MaxChelator software (Patton et al., 2004; http://www.standford.edu/~cpatton/maxc.html). The pH was adjusted to 7.0 with 2-[N-morpholino]ethanesulfonic acid. To compare the channel characteristics accurately, an identical set of intracellular solutions was used throughout the experiments. Commercial software packages, which included Clampex 8.0 or 8.1 (Axon Instruments) and Origin 6.1 (OriginLab Corp., USA), were used for the acquisition and analysis of macroscopic recording data.

Data analysis

To obtain the concentration-response curve of the effect of Rg_3 or TEA on the K^+ currents from the BK_{Ca} channel, the peak amplitudes at different concentrations of Rg_3 or TEA were plotted. The current enhancements or inhibitions evoked by drug treatment were analyzed after subtraction of currents elicited by H_2O injection. Origin software (Origin, USA) was used to fit the plot to the Hill equation: $y/y_{max} = [A]^{nH}/([A]^{nH} + [EC_{50}]^{nH})$, where y represented the peak current at a given concentration of Rg_3, y_{max} was the maximal peak current, EC_{50} was the concentration of Rg_3 producing a half-maximal effect, [A] was the concentration of Rg_3, and nH was the Hill coefficient. All values were presented as mean $\pm$ S.E.M. The significance of differences between mean control and treatment values was determined using Student's *t*-test, where $P < 0.05$ was considered statistically significant.

RESULTS

Treatment of Rg_3 enhances BK_{Ca} channel currents in *Xenopus* oocytes expressing rat brain BK_{Ca} channels

Application of a voltage step from -80 to +40 mV with duration of 400 ms at 10-s intervals to oocytes injected with cRNA encoding the BK α subunit gene elicited a large outward current in the absence of Rg_3 (Fig. 2A, *inset*). Charybdotoxin and Iberiotoxin, highly specific peptidyl inhibitors of maxi-K channels

A

Ginsenosides	R1	R2	R3
Rb₁	-Glc₂-Glc	-H	-Glc₆-Glc
Rc	-Glc₂-Glc	-H	-Glc₆-Ara(fur)
Re	-H	-O-Glc2-Rha	-Glc
Rh₁	-H	-O-Glc	-H
Rf	-H	-O-Glc2-Glc	-H
Rg₁	-H	-O-Glc	-Glc
Rg₃	-Glc₂-Glc	-H	-H

B

BKCa   332 FQNNQALTYWECVYLLMVTMST VGYG DVYAKT 363

KCNQ1   TT IGYG DKVP

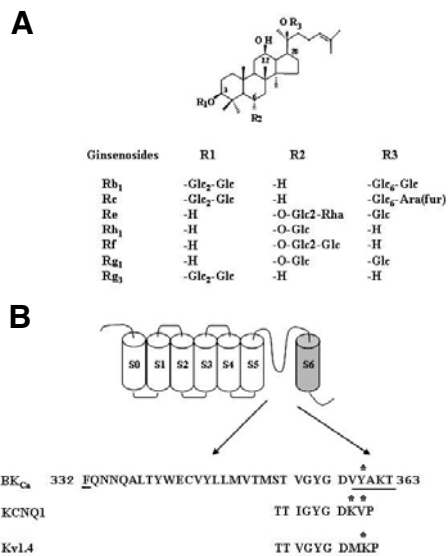Kv1.4   TT VGYG DMKP

Fig. 1. Chemical structures of ginsenosides and the primary amino acid sequence of mutated BK$_{Ca}$ subunit. (A) Structures of ginsenosides. Abbreviations for carbohydrates are as follows: Glc, glucopyranoside; Ara (pyr), arabinopyranoside; Rha, rhamnopyranoside. The subscript indicates the carbon in the glucose ring that links the two carbohydrates. (B) The brief sequence alignment of BK$_{Ca}$ channel and the mutated amino acid residues (underlined) in the pore helix. Amino acid residues in BK$_{Ca}$, KCNQ1, and Kv1.4 channels that were proposed to interact with 20(*S*)-ginsenoside Rg$_3$ (Rg$_3$) are marked (*) amino acid.
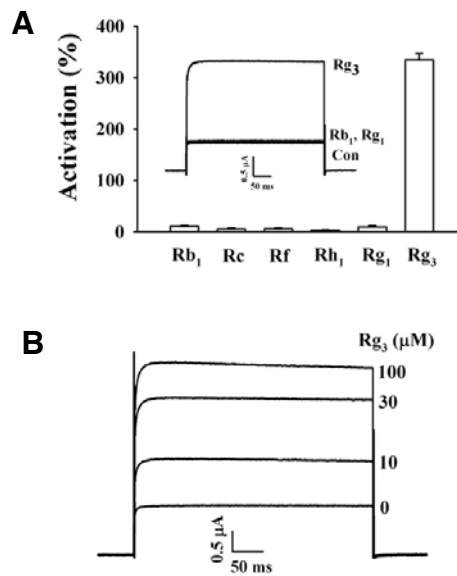
A

B

Fig. 2. Effects of Rg$_3$ on wild-type BK$_{Ca}$ channel activities. (A) Effects of various ginsenosides (100 μM each) on wild-type BK$_{Ca}$ channel currents. *Inset*, the representative traces elicited by ginsenoside Rb$_1$, Rg$_1$ and Rg$_3$. (B) The representative traces on BK$_{Ca}$ channel current enhancements by different concentrations of Rg$_3$ (0, 10, 30 or 100 μM). Rg$_3$ enhanced BK$_{Ca}$ channel current in a concentration-dependent manner. Currents were in response to 400 ms voltage steps to +40 mV from a holding potential of -80 mV. Data represented the mean ± S.E.M. (n = 6-7).

(Candia et al., 1992; Gao et al., 2003), blocked the outward currents (98.2 ± 1.2 and 95.5 ± 2.1% inhibition by 100 nM charybdotoxin and iberiotoxin, respectively, n = 5), indicating that the BK$_{Ca}$ channel is functionally working (Kaczorowski et al., 1996). Next, we examined the effects of various individual ginsenosides on the BK$_{Ca}$ channel currents in *Xenopus* oocytes expressing BK$_{Ca}$ channel α subunits (Fig. 1A). Rg$_3$ (100 μM) activated the BK$_{Ca}$ channel currents by an average of 340%, and other ginsenosides (Rb$_1$, Rc, Rf, Rh$_1$, and Rg$_1$) were much less effective (Fig. 2A). As shown in Fig. 2B, application of Rg$_3$ to oocytes injected with rSlo cRNAs resulted in a rapid stimulation of outward BK$_{Ca}$ channel currents in a concentration-dependent manner. However, Rg$_3$ had no effect on H$_2$O-injected control oocytes that were not injected with cRNA encoding the BK α subunit gene. Thus, the outward currents in H$_2$O-injected control oocytes were 130 ± 25 and 131 ± 10.2 nA in the absence and presence of Rg$_3$, respectively (n = 4). In addition, in oocytes expressing α subunit alone, Rg$_3$ (100 μM) enhanced BK$_{Ca}$ channel currents to a degree similar to that observed in oocytes co-expressing α and β subunits (350 ± 80.6% for α subunit alone; 367 ± 83.1% for α + β subunits, n = 4), indicating that Rg$_3$-mediated enhancement of BK$_{Ca}$ channel currents is independent of β subunit. These results indicated that Rg$_3$ is most potent among various ginsenosides in enhancing BK$_{Ca}$ channel currents.

Rg$_3$-enhancement of BK$_{Ca}$ channel currents was not desensitized by repeated application and was independent of intracellular Ca^{2+}

We next examined the possible changes of Rg$_3$ effect on BK$_{Ca}$ channel currents by repeated application of Rg$_3$ to oocytes expressing BK$_{Ca}$ channel. As shown in Fig. 3A, treatment with

Rg$_3$ induced an enhancement of BK$_{Ca}$ channel currents. Oocytes stimulated with Rg$_3$ were first washed with recording buffer for 3 min until the basal current was recovered, and then re-stimulated with Rg$_3$. The second, third, or fourth BK$_{Ca}$ current responses for Rg$_3$ were not significantly diminished and the magnitudes of BK$_{Ca}$ currents were 94.8 ± 10.3, 78.7 ± 15.4 and 81.0 ± 9.3 % respectively, of the first responses of Rg$_3$ (n = 15, oocytes from three different batches of donors) (Fig. 3B). In addition, we also examined the effect of BAPTA-AM, a cell permeable intracellular Ca^{2+} chelator, on Rg$_3$ enhancement of BK$_{Ca}$ channel currents to investigate whether Rg$_3$ enhancement of BK$_{Ca}$ channel currents was due to the increase of intracellular free Ca^{2+} levels. As shown in Figs. 3C and 3D, pretreatment of BAPTA-AM (10 μM, 3 h) to oocytes had no affect Rg$_3$-mediated BK$_{Ca}$ channel currents. Rather, Rg$_3$ enhanced BK$_{Ca}$ channel currents with concentration-dependent manner, indicating that Rg$_3$-mediated enhancement of BK$_{Ca}$ channel currents is not desensitized and independent of intracellular Ca^{2+}.

The presence of Rg$_3$ caused a rightward shift of TEA-mediated concentration curve on BK$_{Ca}$ channel currents and *vice versa*

Since we demonstrated in the previous report that the regulatory effects of Rg$_3$ on human Kv1.4 channel currents expressed in *Xenopus* oocytes was affected by extracellular application of TEA (Lee et al., 2008), we first examined the effects of TEA on BK$_{Ca}$ channel currents. As shown in Fig. 4A, in wild-type channels, TEA inhibited BK$_{Ca}$ channel currents in a concentration-dependent manner. We next examined Rg$_3$ effects on TEA-mediated inhibition of BK$_{Ca}$ channel currents. Interestingly, the presence of Rg$_3$ (30 μM) caused a rightward shift of the TEA concentration curve on BK$_{Ca}$ channel current inhibi-
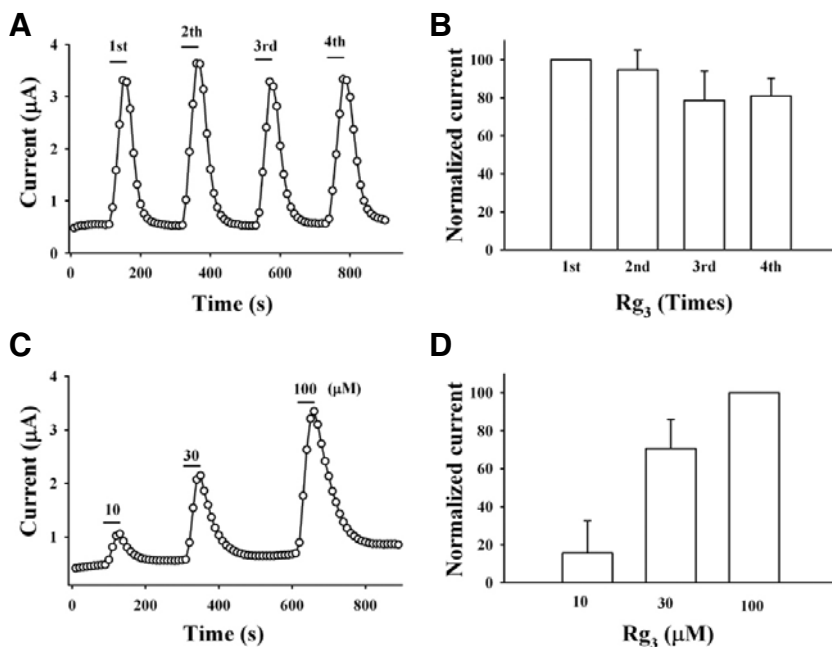
Fig. 3. Rg_3-mediated BK_{Ca} channel current enhancements were not desensitized and were independent of intracellular Ca^{2+}. (A) The representative peak outward current amplitude at +40 mV from a holding potential of -80 mV was measured and plotted against time before and after repeated applications of Rg_3 (100 μM) for 30 s. (B) The normalized currents after repeated Rg_3 treatment. BK_{Ca} channel currents were not desensitized after repeated treatment of Rg_3. Data represented the mean ± S.E.M. (n = 6). (C) Oocytes were first treated with BAPTA-AM (10 μM, 3 h). The representative peak outward current amplitude at +40 mV from a holding potential of -80 mV was measured and plotted against time before and after repeated applications of the indicated concentration of Rg_3. (D) The normalized currents after treatment of various concentrations of Rg_3 in oocytes pre-treated with BAPTA-AM. Data represented the mean ± S.E.M. (n = 6).
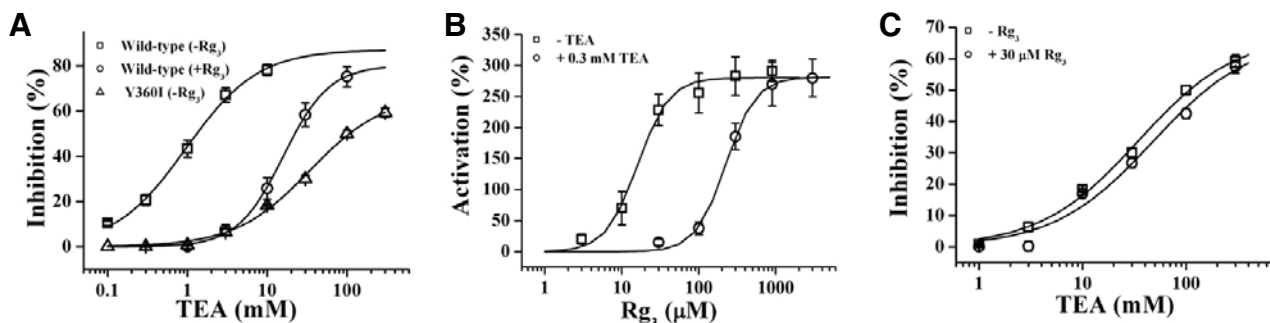

Fig. 4. Effect of TEA on Rg_3 action and *vice versa* in wild-type channel and Y360I mutant effects on TEA and Rg_3 action. (A) Concentration-response curves for TEA in the absence or presence of Rg_3 (30 μM) in wild-type BK_{Ca} channels. The presence of Rg_3 caused a significant rightward shift of TEA concentration-response curves from $0.9 ± 0.1$ to $20.1 ± 2.3$ mM ($p < 0.001$, compared to the absence of Rg_3). In addition, mutation of Y360 to Y360I in the absence of Rg_3 shifted TEA concentration-response curve rightward from $0.9 ± 0.1$ to $34.2 ± 2.6$ mM ($p < 0.001$, compared to wild-type). (B) Concentration-response curves for Rg_3 in the presence of TEA (300 μM) in wild-type BK_{Ca} channels. The presence of TEA caused a significant rightward shift of Rg_3 concentration-response curves from $16.0 ± 1.8$ to $224.2 ± 13.9$ μM ($p < 0.001$, compared to the absence of TEA). (C) Effect of Rg_3 on TEA concentration-response curve in Y360I mutant channel. Rg_3 almost had no effect on TEA concentration-response curve in Y360I mutant channels. Data represented the mean ± S.E.M. (n = 8).

tions from $0.8 ± 0.5$ to $20.1 ± 2.3$ mM ($p < 0.001$, compared to the absence of Rg_3) (Fig. 4A). Second, we examined the effects of TEA on Rg_3-mediated enhancement of BK_{Ca} channel currents. The presence of TEA (300 μM) caused a rightward shift of the Rg_3-mediated concentration curve on BK_{Ca} channel currents from $16.0 ± 1.8$ to $224.2 ± 13.8$ μM ($p < 0.001$, compared to the absence of TEA) (Fig. 4B). In experiments using TEA, our results indicated that Rg_3 enhancement of BK_{Ca} channel currents is achieved through interaction from the outside of the cell.

The pore entryway of channel is involved in Rg_3-mediated enhancement of BK_{Ca} channel currents
Since Rg_3 regulates human Kv1.4 and KCNQ1 plus KCNE1 channels through interaction with amino acids at the channel pore entryway (Choi et al., 2010; Lee et al., 2008), we subsequently examined the possibility of whether Rg_3-induced regulations of BK_{Ca} channel activity were also mediated through inter-

actions with the analogous amino acids from Tyr360 to The363 in the pore entryway (Fig. 1B). The mutants constructed are listed in Table 1. Since mutation Y360A attenuated Rg_3-induced enhancement of BK_{Ca} channel currents (Table 1), we further substituted Y360 with other amino acid residues, including glutamine, isoleucine, lysine, serine, and valine (generating Y360Q, Y360I, Y360K, Y360S and Y360V, respectively), and examined the effect of Rg_3 on BK_{Ca} channel currents in oocytes expressing these mutants. Our results revealed that mutation Y360I greatly attenuated Rg_3-induced enhancement of BK_{Ca} channel currents (Figs. 5A and 5B) and was followed by order of Y360S > Y360E > Y360A. These results indicate that substitutions of Y360 with amino acid residues such as alanine, isoleucine, serine, or glutamate attenuate the Rg_3-induced enhancement of BK_{Ca} channel currents compared to wild-type. However, substitution of other amino acid residues in other positions such as charybdotoxin binding site (F332A) had no discernable effects (Gao et al., 2003, Table 1).

Table 1. Effect of Rg_3 on wild-type and various mutant BK_{Ca} channels expressed in *Xenopus laevis* oocytes. Currents were elicited by single-step voltage pulses from -80 to +40 mV.

	I_{max}			EC_{50}			n_H		
Wild-type	370.4	±	35.1	15.1	±	3.1	1.7	±	0.5
F332A	371.4	±	52.4	41.6	±	13.7	2.7	±	1.9
V359A	641.3	±	67.9	26.8	±	7.4	1.4	±	0.5
Y360A	287.2	±	12.8[#]	43.8	±	4.5*	2.5	±	0.4
Y360I	93.4	±	0.1*	46.8	±	0.1*	1.1	±	0.0
Y360K	409.6	±	29.9	15.5	±	2.6	1.4	±	0.2
Y360Q	440.0	±	36.4	16.4	±	3.2	1.3	±	0.2
Y360S	181.8	±	27.5*	34.4	±	10.7[#]	1.3	±	0.3
Y360V	598.0	±	97.5	43.9	±	17.2*	1.5	±	0.6
Y360E	214.2	±	25.9*	13.6	±	3.4	2.5	±	1.3
A361T	373.9	±	43.4	14.7	±	3.3	1.2	±	0.3
K362A	341.1	±	57.6	12.5	±	3.0	1.1	±	0.2
T363A	311.1	±	45.9	15.0	±	1.0	2.2	±	0.2

I_{max} (%), maximal activation by Rg_3. Rg_3 activation was determined as the % difference of currents in the presence and absence of Rg_3. EC_{50}, Values were mean ± S.E.M (n = 8-10/group). n_H, Hill coefficient. [#]$p <$ 0.05, *$p <$ 0.01 compared with the wild-type BK_{Ca} channel.

Mutation of Y360 to Y360I caused TEA concentration-response curve to rightward shift and abolished Rg_3 effects on TEA concentration-response curve observed in wild-type channel

Interestingly, the previous report showed that Y308 residue of Drosophila BK_{Ca} (*dSlo*) channel is the extracellular TEA binding site and that mutation of Y308 to Y308V almost abolished TEA sensitivity (Shen et al., 1994). Similarly, mutation of Y360, which is the analogous amino acid of Y308 residue of Drosophila BK_{Ca} (*dSlo*) channel, to Y360I also caused a shift of the TEA concentration response curve towards the right and we measured IC_{50} values of 0.9 ± 0.1 and 34.2 ± 2.5 mM ($p <$ 0.001, compared to wild-type) in wild-type and Y360I mutant, respectively (Fig. 4A). In addition, we examined Rg_3 effects on TEA-mediated BK_{Ca} channel regulation using Y360I mutant channel. As shown in Fig. 4C, Rg_3 had almost no effect on TEA-mediated inhibition of mutant BK_{Ca} channel currents. These results indicated that mutation of Y360 to Y360I caused a loss of Rg_3 effects on TEA-mediated BK_{Ca} channel regulations (Lagrutta et al., 1998), again showing a possibility that Rg_3 enhanced BK_{Ca} channel currents by sharing the extracellular TEA binding site of the channel.

Rg_3 activated wild-type but not mutant Y360I BK_{Ca} channels in outside-out configuration

Since Rg_3 enhanced BK_{Ca} channel currents, we next examined Rg_3 effects on BK_{Ca} channel currents using outside-out patch clamp configuration in wild-type and Y360I mutant channels. In current-voltage (I-V) relationships the application of 10 μM Rg_3 slightly enhanced wild-type BK_{Ca} channel currents but the application of 30 μM Rg_3 caused a large enhancement of wild-type BK_{Ca} channel currents (Fig. 6A, right panel). However, in mutant Y360I channels, the enhancing effect of Rg_3 (30 μM) was greatly attenuated (Fig. 6B, right panel). The G-V relationship was also constructed for Rg_3 action in wild-type and Y360I mutant channels. In the absence of Rg_3 the half-activation voltage ($V_{1/2}$) was 136.4 ± 0.4 mV. The presence of 10 and 30 μM Rg_3 caused a shift of $V_{1/2}$ to 123.3 ± 0.3 and 96.30 ± 0.4 mV
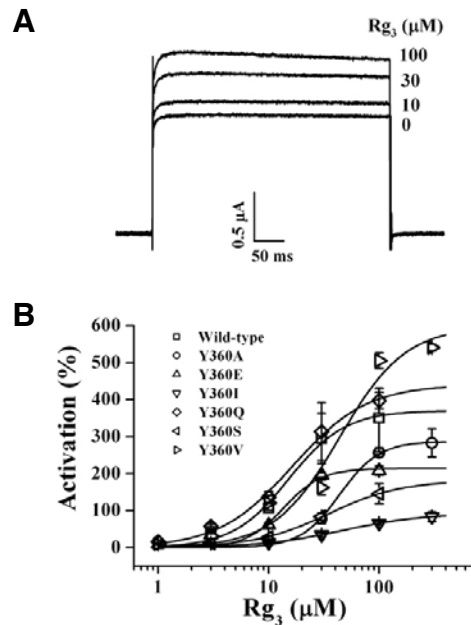
Fig. 5. Effects of Rg_3 on mutant BK_{Ca} channel activities. (A) The representative traces on Rg_3-mediated BK_{Ca} channel current enhancement in Y360I mutant BK_{Ca} channels. Rg_3 slightly enhanced Y360I channel currents. (B) Concentration-response curves of Rg_3 on wild-type and various mutant BK_{Ca} channel currents at Y360 residue. The representative outward current was measured from an oocyte injected with cRNAs that encoded BK_{Ca} channel wild-type or mutant α subunit. Solid lines have been fitted to the Hill equation. Currents were in response to 400 ms voltage steps to +40 mV from a holding potential of -80 mV. Data represented the mean ± S.E.M. (n = 6-7).

in wild-type, respectively (n = 5, $p <$ 0.05, compared to the presence of 30 μM Rg_3). In Y360I mutant channels, $V_{1/2}$ was 140.4 ± 0.4 mV in the absence of Rg_3. The presence of 10 and 30 μM Rg_3 did not cause a significant shift of $V_{1/2}$ to 131.8 ± 0.5 and 120.0 ± 1.0 mV, respectively (n = 5) (Figs. 6C and 6D). These results again indicate that Rg_3 activates BK_{Ca} channels by inducing more negative shift of voltage-activation profile and that mutation of Y360 to Y360I attenuates Rg_3 action.

DISCUSSION

In the nervous system, stimulations above threshold by various stimuli cause activation of voltage-dependent Ca^{2+} channels that induce an elevation of $[Ca^{2+}]_i$ and its resulting elevation initiates signaling pathways for the release of a variety of neurotransmitters from presynaptic sites and Ca^{2+}-dependent cellular events (Hille, 2001). In addition to the role as a second messenger, the elevation of $[Ca^{2+}]_i$ in presynaptic sites is also coupled to activation of BK_{Ca} channels, which are usually co-localized with voltage-dependent Ca^{2+} channels in presynaptic sites for repolarization or return to resting membrane potential (Berkefeld et al., 2006). Thus, since BK_{Ca} channels play a negative feedback control with $[Ca^{2+}]_i$, BK_{Ca} channel activators or openers could be utilized as neuroprotective agents against excessive Ca^{2+} influx through depolarization or excitatory neurotransmitters (Lawson, 2000). Although BK_{Ca} channels are involved in synaptic regulation in the nervous system, relatively little has been studied about the molecular mechanisms by
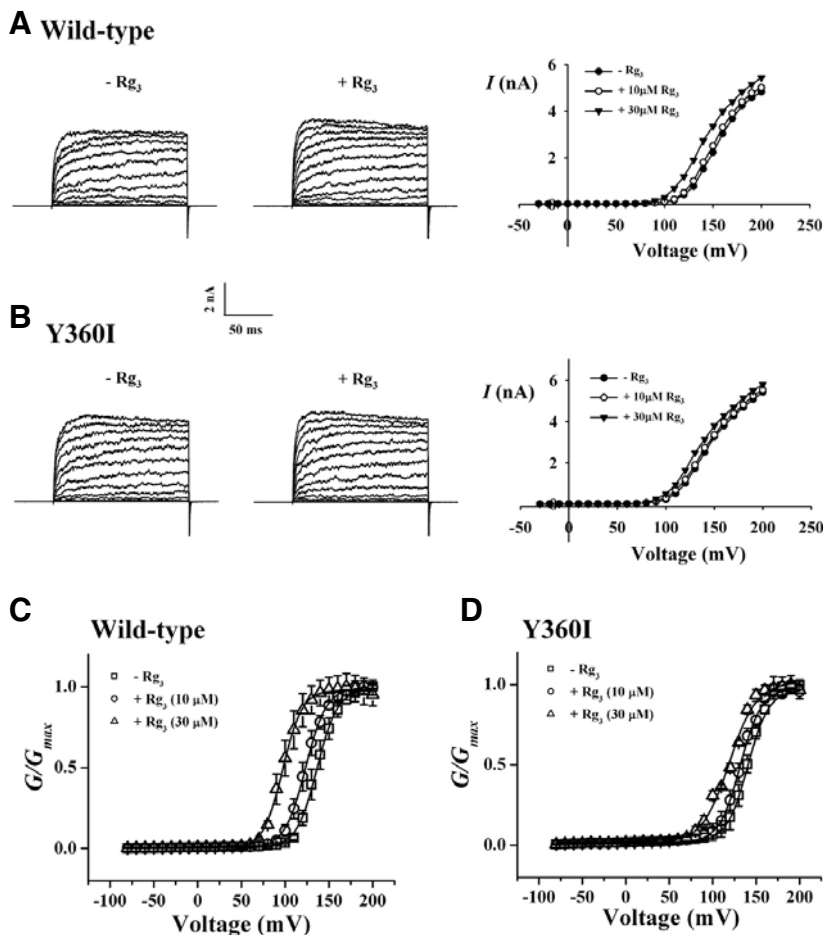
A Wild-type

B Y360I

C Wild-type

D Y360I

Fig. 6. Effects of Rg_3 on wild-type and Y360I mutant BK_{Ca} channel currents in outside-out patch clamp configuration. (A and B) Effects of 30 μM Rg_3 on the macroscopic I-V relationship of wild-type and Y360I mutant BK_{Ca} channel in the presence of 1 μM Ca^{2+}. Representative current traces of macroscopic wild-type (A) or Y360I mutant (B) BK_{Ca} channel currents. Their respective concentrantion-dependent I-V relationships are shown in right panel for wild-type and Y360I mutant channels. Ionic currents were elicited with 200-ms step-pulses of different voltage protocols: -30 to 200 mV in 10-mV increments from holding potentials of -50 mV. Each data point in I-V relationships represents the mean current value measured over 198 ± 1.5 ms of test pulses. (C and D) Effects of Rg_3 on the G-V relationships of wild-type (C) or Y360I mutant (D) BK_{Ca} channel currents. Conductance values were obtained from peak tail currents and normalized to the maximum conductance observed at 10 and 30 μM Rg_3. $V_{1/2}$ values were obtained by fitting independent data sets with Boltzmann function. Each symbol represents the conduc-tance values obtained from two different concentration of Rg_3. Each data point represents the mean value ± S.E.M. (*n* = 5-6 each).

which ginsenosides regulate BK_{Ca} channel activity.

In the present study, we made three major findings. First, we observed that Rg_3 among various ginsenosides enhanced BK_{Ca} channel currents in concentration- and voltage-dependent manners, while Rg_3-enhancement of BK_{Ca} channel currents was independent of intracellular Ca^{2+}. Second, the presence of TEA significantly shifted the concentration response curve of Rg_3 towards the right and *vice versa* in wild-type channel. And third, mutation of the channel pore entry site (Y360 to Y360I), which is also known as extracellular TEA binding site, greatly attenuated Rg_3 enhancement of BK_{Ca} channel currents and caused a rightward shift of the TEA concentration-response curve similar to Rg_3, indicating that Rg_3 may interact with the external TEA biding site via residue Tyr360.

BK_{Ca} channels consist of α and β subunits. The four α subunits assemble to form the channel pore and the auxiliary β subunits function to provide the biophysical and pharmacological properties of channels, including Ca^{2+} and voltage sensitivity, and gating kinetics (Ha et al., 2006; Qian et al., 2002; Valverde et al., 1999; Wallner et al., 1999; Xia et al., 1999). Some BK_{Ca} channel openers such as NS-1619, BMS-204352 and TIBC act independently from the β subunit (Coghlan et al., 2001; Dick et al., 2002; Ha et al., 2006; Imaizumi et al., 2002; Valverde et al., 1999; Vergara et al., 1998), whereas other openers such as dehydrosoyasaponin-I and 17-β-estradiol require β subunit for their action (Giangiacomo et al., 1998; Valverde et al., 1999). In the present study, we found that the Rg_3-enhancement of BK_{Ca} channel current was independent of β subunit

(Fig. 2), suggesting that Rg_3 effects on BK_{Ca} channel are achieved through interaction with α subunit.

Therefore, we next sought to examine the possible mechanisms by which Rg_3 achieved the enhancement of BK_{Ca} channel currents through interaction with α subunit. As shown in Fig. 1A, Rg_3 is a type of glycoside and consists of a carbohydrate portion, a steroid backbone and an alkene side chain (Lee et al., 2008). In a previous report we demonstrated using homology modeling methods that carbohydrate portions of Rg_3 form hydrogen bonds and maintain stable interactions with amino acids of channel proteins (Lee et al., 2008). In addition, we also demonstrated that Rg_3 inhibits Kv1.4 channel currents through interaction with K531 residue, which is located at the channel pore entryway and is also one of the extracellular TEA binding and K^+ activation sites. In contrast, Rg_3 activates KCNQ + KCNE channel through interaction with Lys and Val residues at channel pore entryway (Choi et al., 2010). Based on previous experimental data (Choi et al., 2010; Lee et al., 2008), we first constructed mutant channels at the channel pore entryway of α subunit and found that Rg_3 effects on BK_{Ca} channel current enhancements were also greatly attenuated in Y360I mutant channels.

We observed some consistent results in Rg_3-mediated K^+ channel regulation experiments. As shown in Fig. 1B, K^+ channels exhibit a common feature in that they all have pore-lining P-loop with a consensus amino acid sequence -TXGYGD- which is called the K^+ channel "signature sequence" (Heginbotham et al., 1992; 1994). These residues, repeated in each of

the four α subunits, form the K^+ selectivity filter. In previous studies, mutations of first or second amino acid after -TXGYGD-abolished Rg_3-mediated inhibition (i.e., Kv1.4 channel) (Lee et al., 2008) or Rg_3-mediated activation (i.e., KCNQ + KCNE) (Choi et al., 2010). These results indicate that Rg_3 interacts with amino acid residues in common interaction regions near the "signature sequence" in subsets of K^+ channels examined.

However, it could not be excluded that the Rg_3 might regulate BK_{Ca} channel activity through allosteric mechanisms. In this case, the mutations introduced in Y360 residue might induce the conformational changes and interfere the interaction of Rg_3 with channel proteins, thus attenuating Rg_3-enhancement of BK_{Ca} channel currents. Taken together, although Y360 residue plays an important role in Rg_3-mediated BK_{Ca} channel activation, further studies will be required to elucidate the detailed mechanisms how Rg_3 regulates BK_{Ca} channels.

In summary, we found that Rg_3 enhances BK_{Ca} channel currents without desensitization after repeated treatment and with a Ca^{2+}-independent manner. We have used site-directed mutagenesis to further characterize the Rg_3 interaction site with BK_{Ca} channel. We found that the Y360 residue at the channel pore entryway of brain BK_{Ca} channel is involved in Rg_3-mediated BK_{Ca} channel regulations. These novel findings provide insight into the molecular basis of the pharmacological effects of ginseng in nervous systems.

ACKNOWLEDGMENTS

REFERENCES

Berkefeld, H., Sailer, C.A., Bildl, W., Rohde, V., Thumfart, J.O., Eble, S., Klugbauer, N., Reisinger, E., Bischofberger, J., Oliver, D., et al. (2006). BK_{Ca}-Cav channel complexes mediate rapid and localized Ca^{2+}-activated K^+ signaling. Science *314*, 615-620.

Candia, S., Garcia, M.L., and Latorre, R. (1992). Mode of action of iberiotoxin, a potent blocker of the large conductance Ca^{2+}-activated K^+ channel. Biophys. J. *63*, 583-590.

Choi, S.H., Lee, J.H., Pyo, M.K., Lee, B.H., Shin, T.J., Hwang, S.H., Kim, B.R., Lee, S.M., Oh, J.W., Kim, H.C., et al. (2009). Mutations Leu427, Asn428, and Leu431 residues within transmembrane domain-I-segment 6 attenuate ginsenoside-mediated L-type Ca^{2+} channel current inhibitions. Biol. Pharm. Bull. *32*, 1224-1230.

Choi, S.H., Shin, T.J., Lee, B.H., Chu, D.H., Choe, H., Pyo, M.K., Hwang, S.H., Kim, B.R., Lee, S.M., Lee, J.H., et al. (2010). Ginsenoside Rg_3 activates human KCNQ1 K^+ channel currents through interacting with the K318 and V319 residues: a role of KCNE1 subunit. Eur. J. Pharmacol. *63*, 138-147.

Coghlan, M.J., Carroll, W.A., and Gopalakrishnan, M. (2001). Recent developments in the biology and medicinal chemistry of potassium channel modulators: update from a decade of progress. J. Med. Chem. *44*, 1627-1653.

Dick, G.M., Hunter, A.C., and Sanders, K.M. (2002). Ethylbromide tamoxifen, a membrane-impermeant antiestrogen, activates smooth muscle calcium-activated large-conductance potassium channels from the extracellular side. Mol. Pharmacol. *61*, 1105-1113

Gao, Y.D., and Garcia, M.L. (2003). Interaction of agitoxin2, charybdotoxin, and iberiotoxin with potassium channels: selectivity between voltage-gated and Maxi-K channels. Proteins *52*, 146-54.

Ghatta, S., Nimmagadda, D., Xu, X., and O'Rourke, S.T. (2006). Large-conductance, calcium-activated potassium channels: struc-

tural and functional implications. Pharmacol. Ther. *110*, 103-116.

Giangiacomo, K.M., Kamassah, A., Harris, G., and McManus, O.B. (1998). Mechanism of maxi-K channel activation by dehydro-soyasaponin-I. J. Gen. Physiol. *112*, 485-501.

Ha, T.S., Lim, H.H., Lee, G.E., Kim, Y.C., and Park, C.S. (2006). Electrophysiological characterization of benzofuroindole-induced potentiation of large-conductance Ca^{2+}-activated K^+ channels. Mol. Pharmacol. *69*, 1007-1114.

Hamill, O.P., Marty, A., Neher, E., Sakmann, B., and Sigworth, F.J. (1981). Improved patch-clamp techniques for high-resolution current recording from cells and cell-free membrane patches. Pflugers Arch. *391*, 85-100.

Heginbotham, L., Abramson, T., and Mackinnon R. (1992). A functional conncetion between the pores of distantly related ion channels as revealed by mutant K+ channels. Science *258*, 1152-1155

Heginbotham, L., Lu, Z., Abramson, T., and Mackinnon R. (1994). Mutations in the K^+ channel signature sequence. Biophys. J. *66*, 1061-1067.

Hille, B. (2001). Ion channels of excitable membranes. Sinauer Associates, Inc., (Sunderland, MA, USA).

Imaizumi, Y., Sakamoto, K., Yamada, A., Hotta, A., Ohya, S., Muraki, K., Uchiyama, M., and Ohwada, T. (2002). Molecular basis of pimarane compounds as novel activators of large-conductance Ca^{2+}-activated K^+ channel α-subunit. Mol. Pharmacol. *62*, 836-846.

Kaczorowski, G.J., Knaus, H.G., Leonard, R.J., McManus, O.B., and Garcia, M.L. (1996). High-conductance calcium-activated potas-sium channels; structure, pharmacology, and function. J. Bioenerg. Biomembr. *28*, 255-267.

Lagrutta, A.A., Shen, K.Z., Rivard, A., North, R.A., and Adelman, J.P. (1998). Aromatic residues affecting permeation and gating in dSlo BK channels. Pflugers Arch. *435*, 731-739.

Lawson, K. (2000). Is there a role for potassium channel openers in neuronal ion channel disorders? Expert. Opin. Investig. Drugs *9*, 2269-2280

Lee, J.H., Jeong, S.M., Kim, J.H., Lee, B.H., Yoon, I.S., Lee, J.H., Choi, S.H., Kim, D.H., Rhim, H., Kim, S.S., et al. (2005). Characteristics of ginsenoside Rg_3-mediated brain Na^+ current inhibition. Mol. Pharmacol. *68*, 1114-1126.

Lee, J.H., Lee, B.H., Choi, S.H., Yoon, I.S., Pyo, M.K., Shin, T.J., Choi, W.S., Lim, Y., Rhim, H., Won, K.H., et al. (2008). Ginsenoside Rg_3 inhibits human Kv1.4 channel currents by interacting with the Lys531 residue. Mol. Pharmacol. *73*, 619-626.

Lu, L., Montrose-Rafizadeh, M., and Guggino, W.B. (1990). Ca^{2+}-activated K^+ channels from rabbit kidney medullary thick ascending limb cells expressed in Xenopus oocytes. J. Biol. Chem. *265*, 16190-16194.

Ohi, Y., Yamamura, H., Nagano, N., Ohya, S., Muraki, K., Watanabe, M., and Imaizumi, Y. (2001). Local Ca^{2+} transients and distribution of BK channels and ryanodine receptors in smooth muscle cells of guinea-pig vas deferens and urinary bladder. J. Physiol. *534*, 313-326.

Patton, C., Thomson, S., and Epei, D. (2004). Some precautions in using chelators to buffer metals in biological solutions. Cell Calcium *35*, 427-431.

Qian, X., Nimigean, C.M., Niu, X., Moss, B.L., and Magleby, K.L. (2002). Slo1 tail domains, but not the Ca^{2+} bowl, are required for the beta 1 subunit to increase the apparent Ca^{2+} sensitivity of BK channels. J. Gen. Physiol. *120*, 829-843.

Salkoff, L., Butler, A., Ferreira, G., Santi, C., and Wei, A. (2006). High-conductance potassium channels of the SLO family. Nat. Rev. Neurosci. *7*, 921-931.

Schreiber, M., and Salkoff, L. (1997). A novel calcium-sensing domain in the BK channel. Biophys. J. *73*, 1355-1363.

Schreiber, M., Yuan, A., and Salkoff, L. (1999). Transplantable sites confer calcium sensitivity to BK channels. Nat. Neurosci. *2*, 416-421.

Shen, K.Z., Lagrutta, A., Davies, N.W., Standen, N.B., Adelman, J.P., and North, R.A. (1994). Tetraethylammonium block of slowpoke calcium-activated potassium channels expressed in Xenopus oocytes. Pflugers Arch. *426*, 440-445.

Toro, L., Wallner, M., Meera, P., and Tanaka, Y. (1998). Maxi-K_{Ca}, a unique member of the voltage-gated K^+ channel superfamily. News Physiol. Sci. *13*, 112-117.

Valverde, M.A., Rojas, P., Amigo, J., Cosmelli, D., Orio, P., Bahamonde, M.I., Mann, G.E., Vergara, C., and Latorre, R. (1999).

Acute activation of Maxi-K channels (hSlo) by estradiol binding to the beta subunit. Science *285*, 1929-1931.

Vergara, C., Latorre, R., Marrion, N.V., and Adelman, J.P. (1998). Calcium-activated potassium channels. Curr. Opin. Neurobiol. *8*, 321-329.

Wallner, M., Meera, P., and Toro, L. (1999). Molecular basis of fast inactivation in voltage and Ca^{2+}-activated K^+ channels: a transmembrane β-subunit homolog. Proc. Natl. Acad. Sci. USA *96*, 4137-4142.

Wanner, S.G., Koch, R.O., Koschak, A., Trieb, M., Garcia, M.L., Kaczorowski, G.J., and Knaus, H.G. (1999). High-conductance calcium-activated potassium channels in rat brain: pharmacology, distribution, and subunit composition. Biochemistry *38*, 5392-400.

Wei, A., Solaro, C., Lingle, C., and Salkoff, L. (1994). Calcium sensitivity of BK-type KCa channels determined by a separable domain. Neuron *13*, 671-681.

Weiger, T.M., Hermann, A., and Levitan, I.B. (2002). Modulation of calcium-activated potassium channels. J. Comp. Physiol. A. Neuroethol. Sens. Neural. Behav. Physiol. *188*, 79-87.

Xia, X.M., Ding, J.P., and Lingle, C.J. (1999). Molecular basis for the inactivation of Ca^{2+}- and voltage-dependent BK channels in adrenal chromaffin cells and rat insulinoma tumor cells. J. Neurosci. *19*, 5255-5264.